

Quantum Computing for X-ray Astronomy

Review, Analysis, and Prospects

Taha Selim

t.i.m.m.selim2@hva.nl

Lecturer/Researcher of Quantum Computing and Quantum Theoretical Chemistry
Amsterdam University of Applied Sciences

November 25th, 2025
SRON Netherlands Institute for Space Research

What we will present today?



Jan Blommaart
Managing Director BioDAC



Taha Selim
Lecturer/Researcher of Quantum Computing
and Quantum Theoretical Chemistry,
Amsterdam University of Applied Sciences

Full team: Jelle de Plaa (SRON), Liyi Gu (SRON), Taha Selim (HvA), Marc Bremer (HvA), Lourens Benningshof (BioDAC), en Jan Blommaart (BioDAC).

Together with SRON team, we explore the potential of quantum computing in providing accurate atomic data and speeding up the spectral modeling codes like SPEX by optimizing atomic data calculations using quantum computing techniques.

Outline

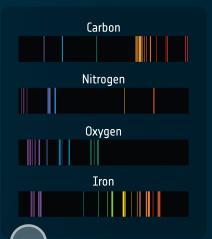
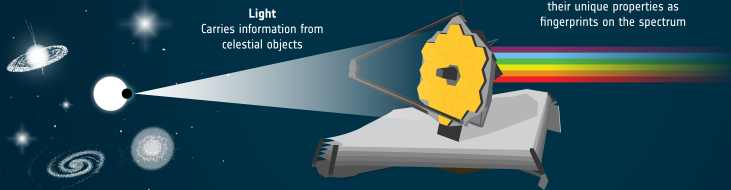
- PhD Work on Infrared Molecular Spectroscopy and Modelling
- X-ray Astronomy Simulations and Black Hole Spin Measurements
- Quantum Computing for Atomic Data Calculations
- Quantum Computing architectures and roadmap

James Webb Space Telescope (JWST)



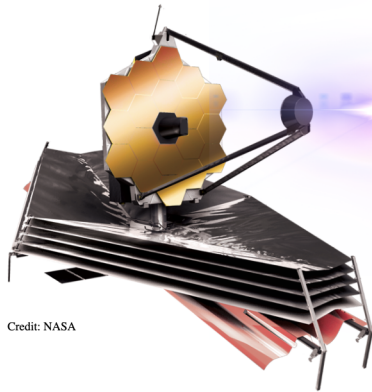
SPECTROSCOPY WITH WEBB

Spectroscopy is a tool that astronomers use to better understand the physics of objects in space. Like a prism splits white light from the Sun into its colour components (like a rainbow), Webb's spectrographs will dissect infrared light into its many wavelengths. This will provide detailed information about an object, such as how a galaxy moves or what molecules are present in an exoplanet's atmosphere.

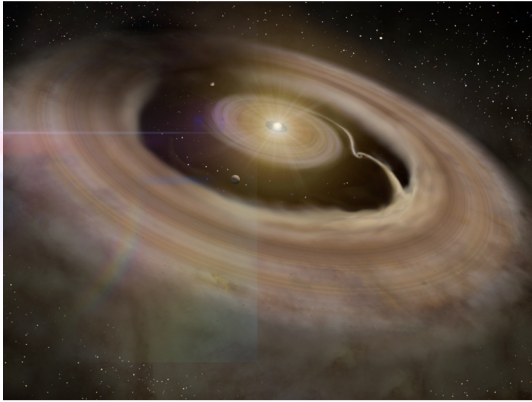


Spectra detectives
Scientists study spectra to analyse what atoms and molecules are present in the source. Spectra also reveal the temperature, density and motion of the objects

James Webb Space Telescope (JWST)



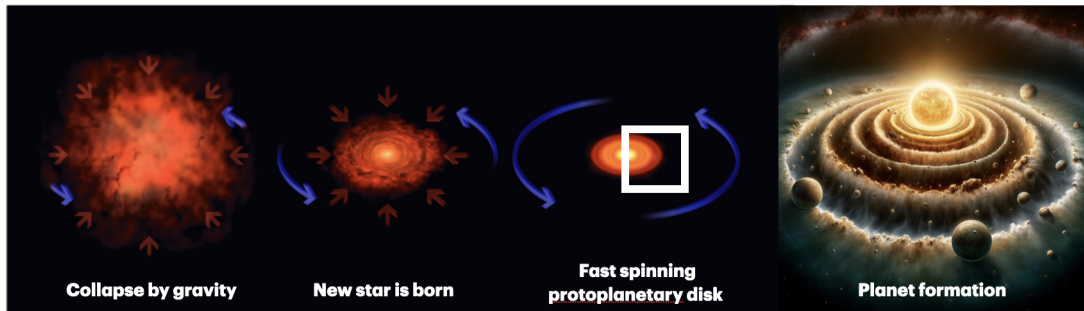
Credit: NASA



Credit: The Graduate University for Advanced Studies/NAOJ

Powerful near and mid-infrared observational capabilities

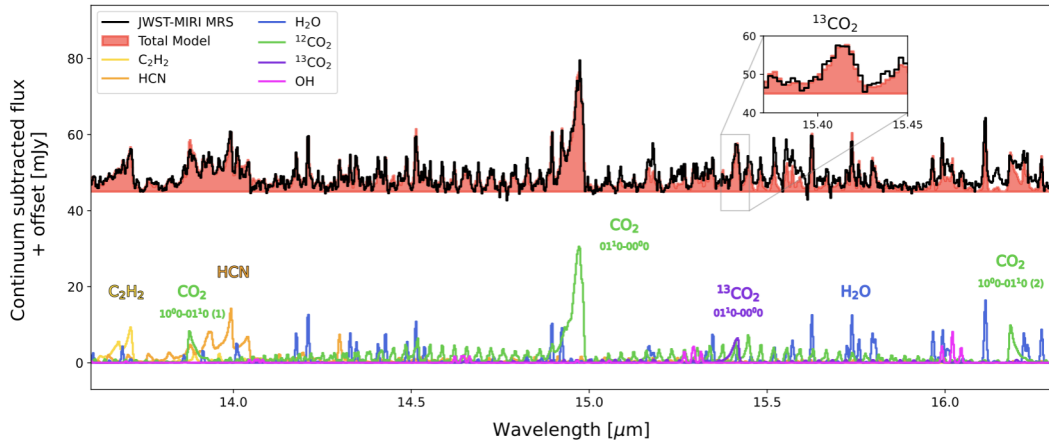
Protoplanetary disks and molecular spectroscopy



Key molecules

CO CO_2 HCN H_2O C_2H_2 CH_4

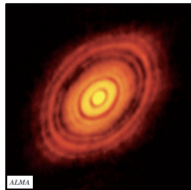
Modelling recorded spectra



Sierra L. Grant, Ewine F. van Dishoeck, et al. 2023 ApJL 947 L6

CO_2 is a key molecule in interstellar media

CO_2 was found in interstellar media and (exo-)planets



Protoplanetary disk T Tauri Star



Venus



Jupiter's moon Europa



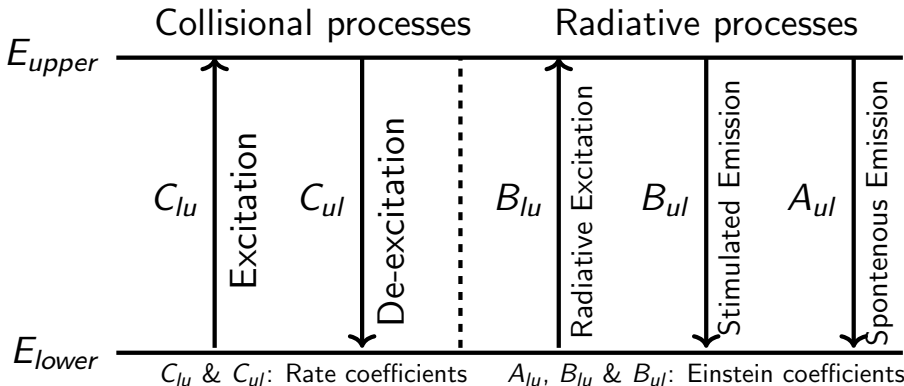
Exoplanet K2-18 b

Illustration Credit: NASA, ESA, CSA, and J. Olmsted (STScI)

Deriving the interstellar molecular abundances

Modeling the observed spectra requires:

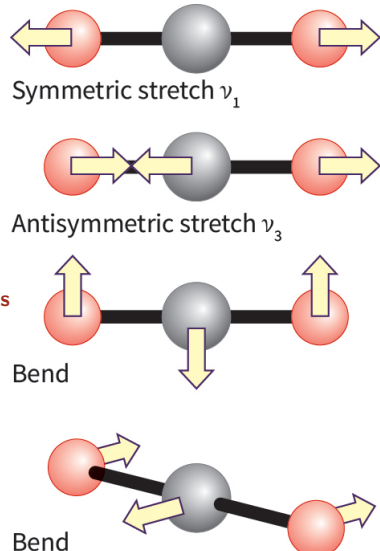
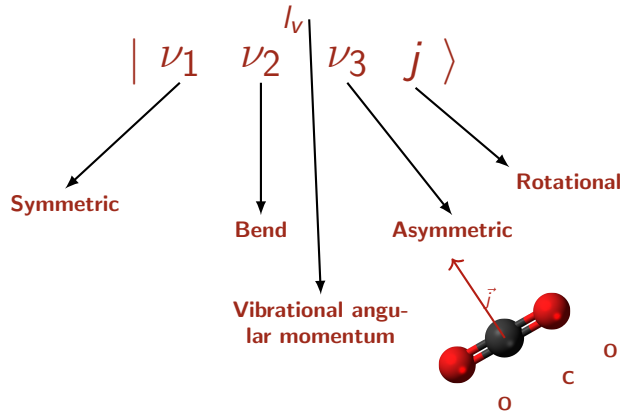
Not in Thermodynamic Equilibrium (Non-LTE) environment modeling



CO_2 Rotational-vibrational states

CO_2 three vibrational modes - two modes are infrared active **Labeling the rovibrational**

quantum state: **5 quantum numbers**



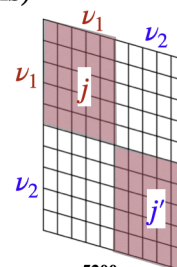
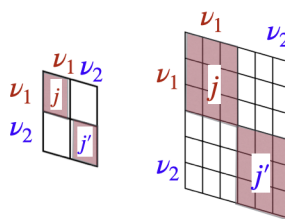
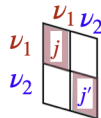
Computational complexity of rovibrational transition rates

Two main challenges, considering CO₂:

- Theoretical formalism and codes to enable the calculations
- Efficient procedures to reduce the computational complexity

$$\text{Time} \propto (\text{Number of coupled equations})^3$$

Single
calculation



Number of coupled equations: ~100

Time (seconds): ~0.5 s

~300

~4.15 s

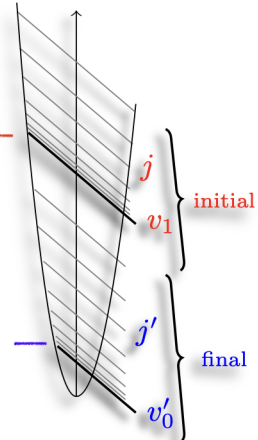
~5200

~6600 s

$|10^0 0 j >$

$|00^0 0 j >$

Example: symmetric stretch

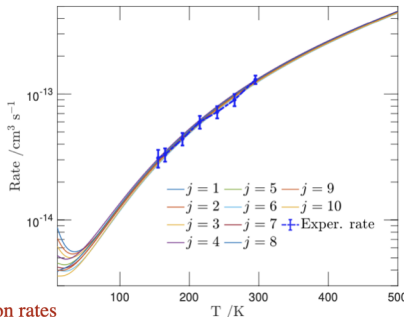


PhD work results

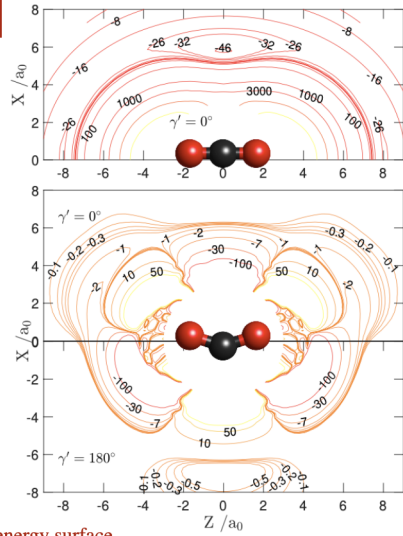
PhD work

Develop theoretical formalisms and codes to calculate rates of collision-induced rovibrational transitions of **CO₂** with **He** atoms.

Calculations: Symmetric, asymmetric, and bend modes



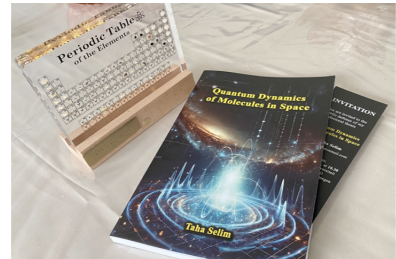
Example,
bend collision rates



Example,
bend potential energy surface

PhD Research Overview

- Taha Selim. (2024). *Quantum dynamics of molecules in space: Theoretical studies and efficient computational methods for collision-induced rovibrational transition rates in molecules*. [Doctoral dissertation, Radboud University].
- Taha Selim, Arthur Christianen, Ad van der Avoird, & Gerrit C. Groenenboom. (2021). Multi-channel distorted-wave Born approximation for rovibrational transition rates in molecular collisions. *The Journal of Chemical Physics*, 155(3), 034105.
- Taha Selim, Ad van der Avoird, & Gerrit C. Groenenboom. (2022). Efficient computational methods for rovibrational transition rates in molecular collisions. *The Journal of Chemical Physics*, 157(6), 064105.
- Taha Selim, Ad van der Avoird, & Gerrit C. Groenenboom. (2023). State-to-state rovibrational transition rates for C_3 in the bend mode in collisions with He atoms. *The Journal of Chemical Physics*, 159(16), 164310.



PhD Thesis Cover Page,
Taha Selim, 2024

Computational complexity of molecular modelling and simulations

- Molecular systems are inherently quantum mechanical, requiring accurate quantum descriptions for properties and dynamics.
- Atomic transitions also cost extensive computational resources to model accurately.
- Multi-electron calculations scale exponentially with the number of electrons.
- Classical computers struggle with simulating quantum systems due to this exponential scaling.
- Quantum computers can potentially simulate quantum systems more efficiently by leveraging qubits and quantum algorithms

X-ray astronomy simulations and black hole spin measurements

X-ray astronomy simulations help in studying underlying physics of the accretion of massive black holes, testing general relativity predictions in strong gravity fields, and measuring black hole spin rates through high-resolution spectroscopy.

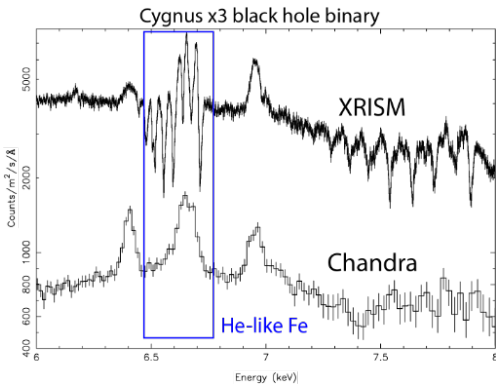
- Investigating the extreme physics of black hole accretion to test predictions of General Relativity in strong gravity fields.
- Identifying the last stable orbit of matter around black holes, known as the Innermost Stable Circular Orbit (ISCO), before falling into the event horizon.
- The ISCO location directly correlates to spin. Rapidly spinning (*Kerr*) black holes pull the ISCO closer to the event horizon than static (*Schwarzschild*) ones.
- XRISM resolves fine spectral features (like Iron lines) distorted by extreme gravity and velocity, allowing precise calculation of spin rates for black holes of all sizes.
- This mission serves as a pathfinder for the upcoming *Athena* telescope (10x sensitivity) and complements future gravitational wave data from *LISA*.



Artist impression of Cygnus X-3. The image illustrates a black hole candidate traversing the dense stellar winds of a Wolf-Rayet companion star. This environment is believed to sustain an accretion disk and launch powerful jets from the black hole. **Photo: NASA**

Computational complexity of x-ray astronomy simulations

- Significant improvement provided by XRISM comparing to Chandra Groundbreaking capabilities in x-ray spectroscopy similar to JWST in infrared and optical wavelengths.
- XRISM significantly outperforms Chandra in spectral resolution for black hole observations, particularly within the He-like Iron band.
- Both spectra are normalized to ensure a direct and accurate comparison.
- The spectra provides quantum level of details aiding the modeling process of the chemical composition of matter around black holes for the first time.
- Athena mission is expected to further enhance the spectra by 10x compared to XRISM.



Comparison of Chandra and XRISM resolution capabilities. [Reference:](#)

Atomic transition rates and level populations

the demand for larger and accurate atomic data to model high-resolution spectra from XRISM and Athena missions.

- Atomic transition rates and level populations are crucial for modeling X-ray spectra from astrophysical sources.
- Computational complexity: Calculating accurate atomic data involves solving complex quantum mechanical equations, which can be computationally intensive.
- Large datasets: High-resolution spectra require extensive atomic databases, leading to increased storage and retrieval challenges.
- Focus on speeding up spectral modeling codes like SPEX by optimizing atomic data calculations using quantum computing techniques.

Reference: [1]

Classical computing vs. quantum computing

Classical bits:

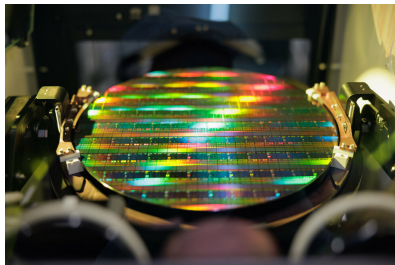
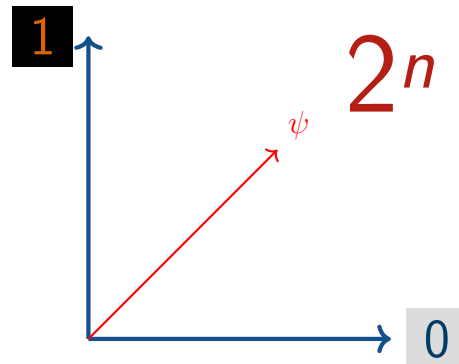


Illustration of a wafer. Photo: ASML

Quantum bits (qubits):

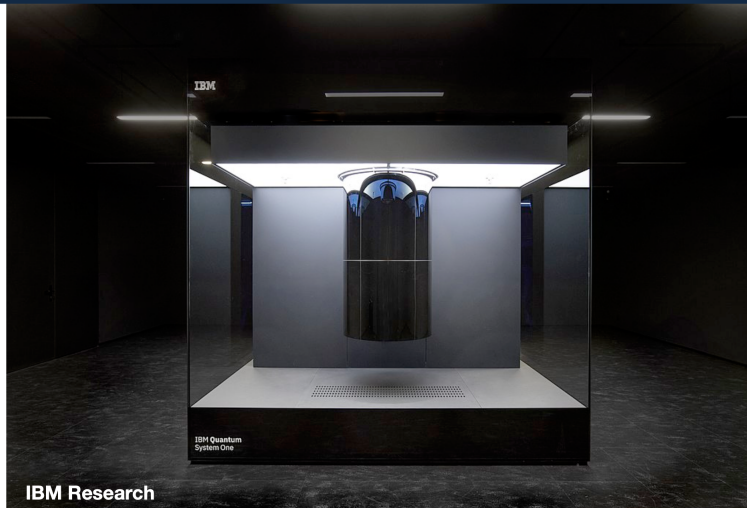


$$\text{Qubit } \square = a \square 0 + b \square 1$$

Bit 0 1

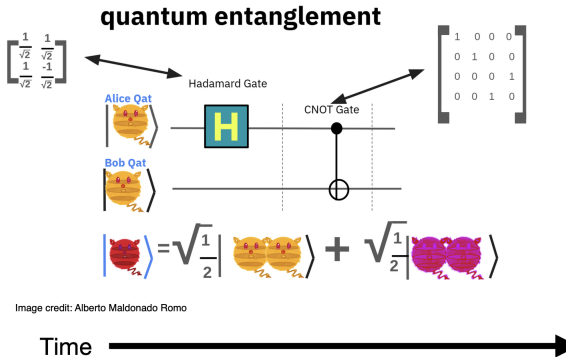
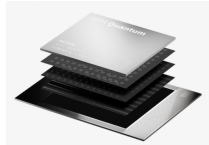
Current quantum computing technologies and architectures

| IBM quantum computer >



Current quantum computing technologies and architectures

A sequence of gates applied to a given quantum register of qubits:



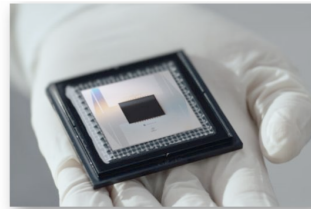
Current quantum computing technologies and architectures

Different types of quantum computing, each has its own mechanism.



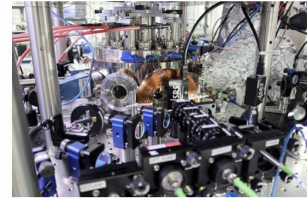
QuiX - <https://www.quixquantum.com/>

Photonic quantum processor



Google, new Willow chip

Superconducting quantum processor



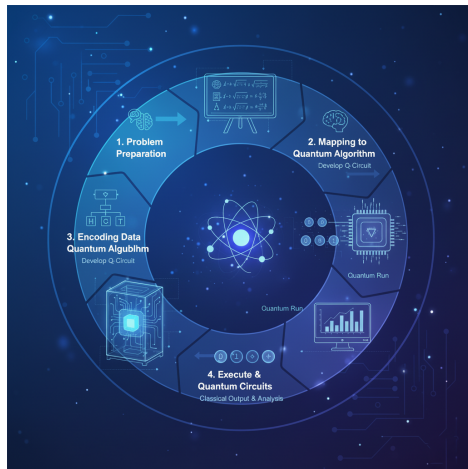
Kenji Ohmori group at the Institute for Molecular Science.
Courtesy of Takafumi Tomita.

Ultracold neutral atoms
quantum processor

Quantum computing workflow

Typical steps in a quantum computing workflow:

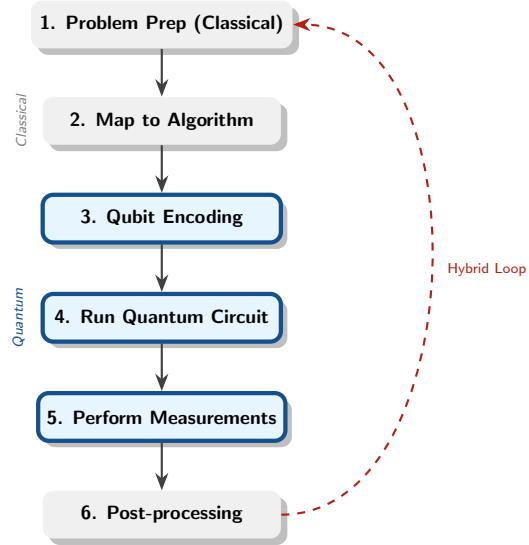
- Problem preparation with a classical algorithm
- Map the problem into a quantum algorithm or a hybrid classical-quantum workflow
- Initial data loading on the quantum register (qubit encoding)
- Translate the quantum algorithm into a quantum circuit and run it
- Perform measurements
- Post-processing



Quantum Computing Workflow

Quantum computing workflow diagram

- **Problem Preparation:**
Define Hamiltonian using classical algorithm.
- **Mapping:**
Convert problem to quantum compatible format (Hybrid workflow).
- **Data Loading:**
Initial state encoding on quantum register (Qubit encoding).
- **Execution:**
Translate algorithm to circuit and run on QPU.
- **Measurement:**
Collapse state and read classical bits.
- **Post-processing:**
Classical analysis of measurement results.



Use Case I: Using HHL for rate solve in SPEX

SPEX is a spectral fitting software package used in X-ray astronomy for modeling and analyzing high-resolution spectra from astrophysical sources. The subroutine `ratesolve.f90` essentially solves the rate equations for a given set of atomic levels.

The equation is implemented in the form of a matrix equation:

$$\underline{R} \cdot \underline{P}_n + \underline{S} = 0.$$

- R is the transition matrix for all possible radiative and collisional processes between levels i and j .
- P_n is the occupation of the energy levels for the ion.
- S contains the source terms (recombinations or ionisations to or from the relevant level).
- This matrix equation is part of bigger loop to include the effect of neighboring ions and update the vector S accordingly.

The computational complexity of solving this matrix equation using classical methods scales as $O(N^2)$, where N is the number of atomic levels involved.

Use Case I: Using HHL for rate solve in SPEX

SPEX is a spectral fitting software package used in X-ray astronomy for modeling and analyzing high-resolution spectra from astrophysical sources. The subroutine `ratesolve.f90` essentially solves the rate equations for a given set of atomic levels.

The equation is implemented in the form of a matrix equation:

$$\underline{R} \cdot \underline{P}_n + \underline{S} = 0.$$

Method	Complexity	Best For
Gaussian Elimination	$\mathcal{O}(N^3)$	Small, dense systems (e.g., $N < 10,000$).
Classical Iterative	$\approx \mathcal{O}(N^2)$	Large, sparse systems (standard simulations).
Quantum HHL	$\mathcal{O}(\text{polylog}(N))$	Massive systems where N is exponentially large, provided the condition number κ is low.

Table: Comparison of Computational Complexity: Classical vs. Quantum Solvers.

HHL: Harrow-Hassidim-Lloyd quantum algorithm for solving linear systems of equations.

HHL algorithm overview

HHL algorithm is a quantum algorithm designed to solve linear systems of equations.
It computes:

$$|\mathbf{b}\rangle \xrightarrow{\text{HHL}} |A^{-1}\mathbf{b}\rangle.$$

where the solution vector $|\mathbf{x}\rangle$ is represented as:

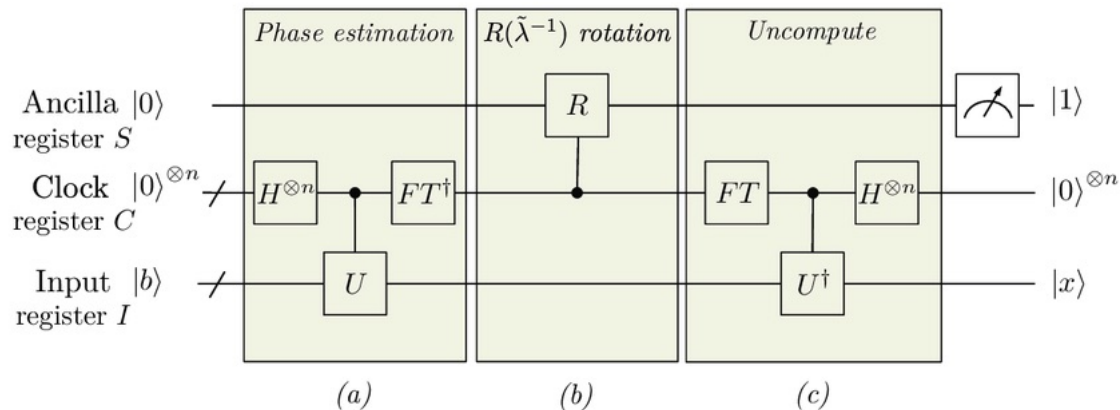
$$|\mathbf{x}\rangle = \frac{\sum_i x_i |i\rangle}{\sqrt{\sum_i |x_i|^2}}, \quad |\mathbf{b}\rangle = \frac{\sum_i b_i |i\rangle}{\sqrt{\sum_i |b_i|^2}},$$

where x_i and b_i are the components of the solution and input vectors, respectively, and $|i\rangle$ denotes the computational basis states corresponding to the binary representation of the index i . For example, $|5\rangle = |0\dots0101\rangle$ [2]. A is a Hermitian matrix, and $|\mathbf{b}\rangle$ is the input state vector.

Key points about HHL's computational complexity:

- Representing a vector of size N requires $\log_2(N)$ qubits.
- Computational complexity of HHL scales as $\mathcal{O}(\text{polylog}(N))$ or about $\mathcal{O}((\log N))$ polynomially, depending on the condition number κ of matrix A .
- HHL is most efficient for large, sparse matrices with low condition numbers.

HHL algorithm steps



Typically, we need to convert a non-Hermitian matrix equation into a Hermitian one to apply HHL. This can be done by constructing an augmented matrix:

$$\tilde{A} = \begin{pmatrix} O & A \\ A^\dagger & O \end{pmatrix}, \tilde{\mathbf{b}} = \begin{pmatrix} \mathbf{b} \\ \mathbf{0} \end{pmatrix}$$

Quantum computing approach

First quantization

$$\hat{H} = \frac{\hat{p}^2}{2m} + \frac{1}{2}m\omega^2\hat{x}^2$$

$$a^\dagger \Psi_n(x) = \sqrt{n+1} \Psi_{n+1}(x)$$

$$a \Psi_n(x) = \sqrt{n} \Psi_{n-1}(x)$$

$$a^\dagger a \Psi_n(x) = n \Psi_n(x)$$

where $\Psi_n(x)$ are the wavefunctions.

Second Quantization

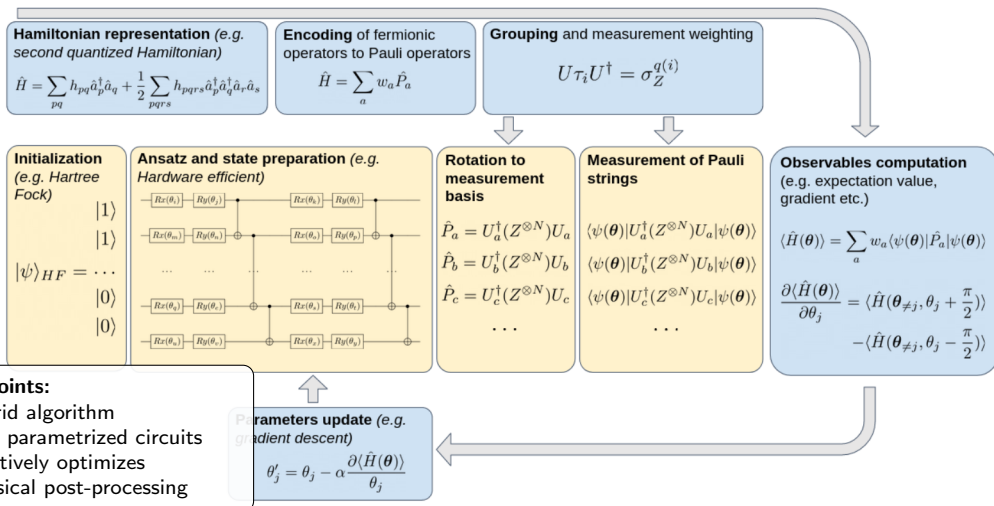
$$\hat{H} = \hbar\omega \left(\hat{a}^\dagger \hat{a} + \frac{1}{2} \right)$$

$$a^\dagger = \sqrt{\frac{m\omega}{2\hbar}} x - i \frac{1}{\sqrt{2m\hbar\omega}} \frac{d}{dx}$$

$$a = \sqrt{\frac{m\omega}{2\hbar}} x + i \frac{1}{\sqrt{2m\hbar\omega}} \frac{d}{dx}$$

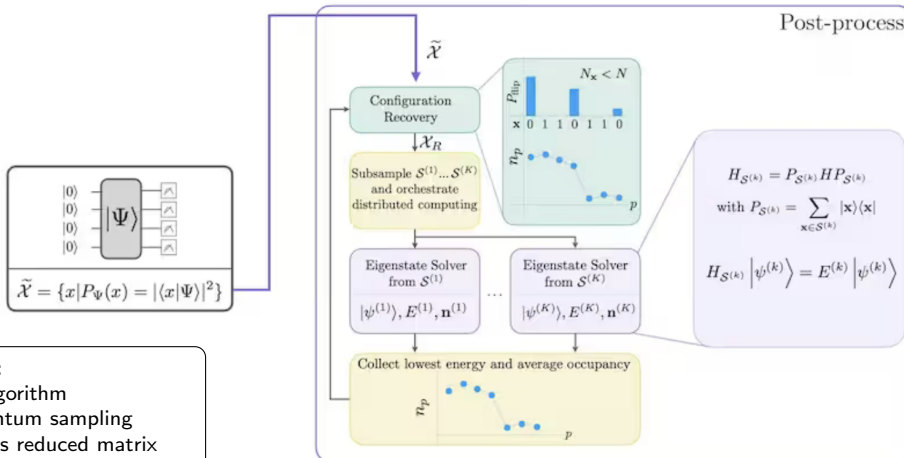
$E_n = (n + \frac{1}{2})\hbar\omega$ are the energy levels
 $n = 0, 1, 2, \dots$ is the quantum number.

Variational Quantum Eigensolver (VQE) approach



VQE algorithm workflow diagram. It is a hybrid quantum-classical algorithm used to find the ground state energy of a quantum system. **Goal: Compute transition probability in He-like Iron in plasma state.**

Sample-based Quantum Diagonalization (SQD) approach



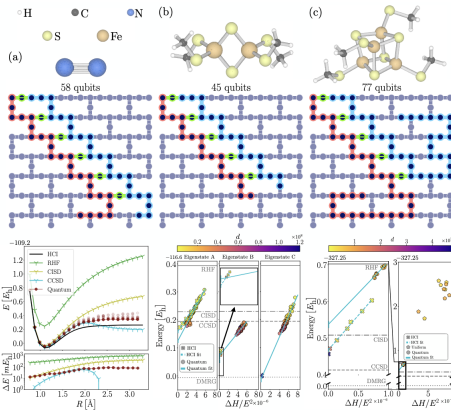
VQE algorithm workflow diagram. It is a hybrid quantum-classical algorithm used to find the ground state energy of a quantum system. **Goal: Compute transition probability in He-like Iron in plasma state.**

Use case I: IBM quantum-centric supercomputing architecture

IBM uses quantum-centric supercomputing architecture to tackle complex quantum chemistry problems: With HPC as Fugaku and QPU as Heron.

Recent IBM work using SQD to use chemistry on large basis set and compute:

- N₂ triple bond dissociation energy: well-known test of the accuracy of electronic structure methods in the presence of static electronic correlation.
- Ground states of Iron-Sulfur (FeS) clusters: The [2 Fe–2 S] cluster and [4 Fe–4 S] cluster, challenging systems for classical methods due to their complex electronic structure and strong electron correlation effects.

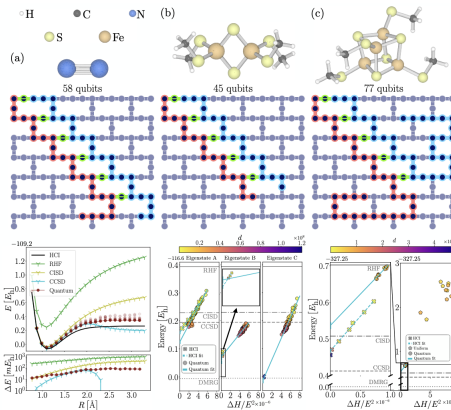


SQD use cases by IBM research team. Reference: [3]

Use case I: IBM quantum-centric supercomputing architecture

Nitrogen Molecule (N_2) Dissociation (6-31G basis)

Metric	Details
Qubits Used	36 total qubits used, with 32 for the Jordan-Wigner (JW) encoding.
Quantum Gates	762 CNOT gates. 1,408 total gates. Circuit depth $d = 148$.
HPC Usage (Classical)	Subspace diagonalization was performed on classical nodes using the PySCF library. A subspace dimension of $d = 4\text{M}$ was used for wavefunction visualization analysis.

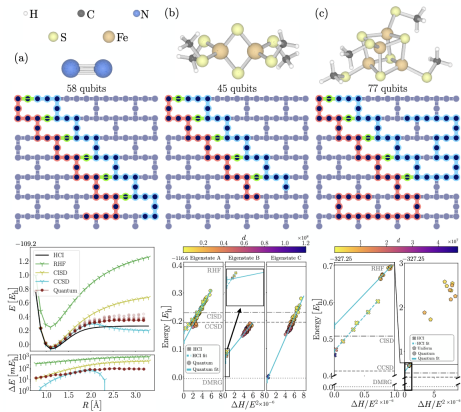


SQD use cases by IBM research team. Reference: [3]

Use case I: IBM quantum-centric supercomputing architecture

Nitrogen Molecule (N_2) Dissociation (cc-pVDZ basis)

Metric	Details
Qubits Used	58 total qubits used, with 52 for the Jordan-Wigner (JW) encoding.
Quantum Gates	1,792 CNOT gates . 3,412 total gates . Circuit depth $d = 223$. The circuit size reached approximately 1–1.5K two-qubit gates .
HPC Usage (Classical)	Used $d = 16 \cdot 10^6$ (16M) configurations for projection and diagonalization. The combined quantum runtime for all points in the dissociation curve was approximately 45 minutes . Classical diagonalization used the PySCF library on a single node.

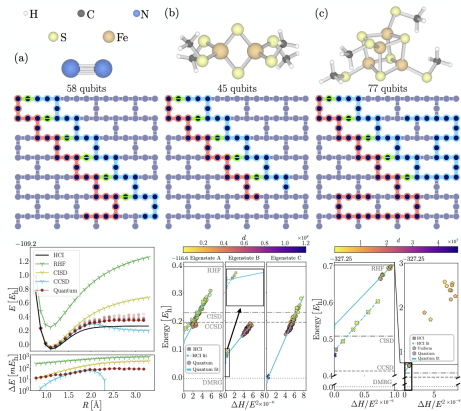


SQD use cases by IBM research team. Reference: [3]

Use case I: IBM quantum-centric supercomputing architecture

[2 Fe–2 S] Cluster Simulation

Metric	Details
Qubits Used	45 total qubits used, with 40 for the Jordan-Wigner (JW) encoding.
Quantum Gates	1,100 CNOT gates . 2,070 total gates . Circuit depth $d = 173$. Circuit sizes reached approximately 1–1.5K two-qubit gates .
HPC Usage (Classical)	Quantum runtime was approximately 45 minutes . Classical diagonalization used the PySCF library on a single node. Vertical scaling analysis showed the optimal configuration for this system required 30+ CPUs per node for the eigenstate solver.



SQD use cases by IBM research team. Reference: [3]

Current projects and future work

Several ongoing projects and future directions aim to further explore and enhance the application of quantum computing in astrophysical simulations:

- optimize computing atomic transition rates and level populations using quantum algorithms to improve the accuracy and efficiency of spectral modeling codes like SPEX.
- Explore leveraging hybrid quantum-classical algorithms to speed up the computation of radiative transfer simulations in astrophysical contexts.
- Investigate the potential of quantum computing to run accurate simulations and provide accurate atomic data for high-resolution X-ray spectra analysis.

Extra use cases

- SQD: Alain Chancé: https://github.com/AlainChance/SQD_Alain
- MolKet's Julia package:

References

- ❑ J. DE PLAA, J. S. KAASTRA, L. GU, J. MAO, and T. RAASSEN,
SPEX: High-Resolution Spectral Modeling and Fitting for X-ray Astronomy, 2019.
- ❑ QULACS DOJO,
7.2 Harrow-Hassidim-Lloyd algorithm,
https://dojo.qulacs.org/en/latest/notebooks/7.2_Harrow-Hassidim-Lloyd_algorithm.html, n.d.,
Accessed: 2025-11-23.
- ❑ J. ROBLEDO-MORENO, M. MOTTA, H. HAAS, A. JAVADI-ABHARI,
P. JURCEVIC, W. KIRBY, S. MARTIEL, K. SHARMA, S. SHARMA,
T. SHIRAKAWA, I. SITDIKOV, R.-Y. SUN, K. J. SUNG, M. TAKITA, M. C.
TRAN, S. YUNOKI, and A. MEZZACAPO,
Science Advances **11** (2025).